BJP BRITISH JOURNAL OF PHARMACOLOGY

BPS BRITISH PHARMACOLOGICAL SOCIETY

British Journal of Pharmacology (2010), 159, 761–771

0007-1188/09
www.brjpharmacol.org

THEMED SECTION: IMAGING IN PHARMACOLOGY

REVIEW

Visualization of gene expression in the live subject using the Na/I symporter as a reporter gene: applications in biotherapy

Patrick Baril[1], Pilar Martin-Duque[2] and Georges Vassaux[1]

[1]*Inserm U948, Université de Nantes, Nantes Atlantique Universités, EA4274, Institut des Maladies de l'Appareil Digestif, CHU Hôtel Dieu, Nantes, France, and* [2]*Investigadora Araid/Instituto Aragonés de CC de la Salud, Avda Gómez Laguna, Zaragoza, Spain*

Biotherapies involve the utilization of antibodies, genetically modified viruses, bacteria or cells for therapeutic purposes. Molecular imaging has the potential to provide unique information that will guarantee their biosafety in humans and provide a rationale for the future development of new generations of reagents. In this context, non-invasive imaging of gene expression is an attractive prospect, allowing precise, spacio-temporal measurements of gene expression in longitudinal studies involving gene transfer vectors. With the emergence of cell therapies in regenerative medicine, it is also possible to track cells injected into subjects. In this context, the Na/I symporter (NIS) has been used in preclinical studies. Associated with a relevant radiotracer ($^{123}I^-$, $^{124}I^-$, $^{99m}TcO4^-$), NIS can be used to monitor gene transfer and the spread of selectively replicative viruses in tumours as well as in cells with a therapeutic potential. In addition to its imaging potential, NIS can be used as a therapeutic transgene through its ability to concentrate therapeutic doses of radionuclides in target cells. This dual property has applications in cancer treatment and could also be used to eradicate cells with therapeutic potential in the case of adverse events. Through experience acquired in preclinical studies, we can expect that non-invasive molecular imaging using NIS as a transgene will be pivotal for monitoring *in vivo* the exact distribution and pharmacodynamics of gene expression in a precise and quantitative way. This review highlights the applications of NIS in biotherapy, with a particular emphasis on image-guided radiotherapy, monitoring of gene and vector biodistribution and trafficking of stem cells.
British Journal of Pharmacology (2010) **159,** 761–771; doi:10.1111/j.1476-5381.2009.00412.x; published online 8 October 2009

This article is part of a themed section on Imaging in Pharmacology. To view the editorial for this themed section visit http://dx.doi.org/10.1111/j.1476-5381.2010.00685.x

Keywords: Na/I symporter; gene transfer; non-invasive molecular imaging; radiotherapy; cell trafficking; biotherapy

Abbreviations: DAB-AM16, Diaminobutane based polypropylenimine dendrimers; GFP, green fluorescent protein; HPMA, N-2-hydroxypropylmethacrylamide; HSV-1-*tk*, the herpes simplex virus thymidine kinase gene; MRI, Magnetic resonance imaging; NIS, Na/I symporter; PEG, Poly(ethylene glycol); PET, Positron emission tomography; SPECT, single photon emission computed tomography; Tg, thyroglobulin; TIFF-1, thyroid transcription factor-1; %ID/g, percentage of injected dose per gram; TRs, thyroid stimulating hormone receptor; TSH, thyroid stimulating hormone

Introduction

The development of technologies allowing the imaging of biological processes in live subjects started 40 years ago and is now in an exponentially growing phase. By definition, molecular imaging is the visual representation and characterization of biological processes at both the cellular and subcellular level (Blasberg, 2003). Applications of molecular imaging technology in biomedicine are large. It can facilitate tumour detection at an early stage for diagnosis (Kelly *et al.*, 2008), provide early information on the efficiency of a treatment (Geus-Oei and Oyen, 2008), offer opportunities to study fundamental biological processes in living animal models

Correspondence: Patrick Baril, Laboratoire de Biothérapie Hépatique, Inserm U948, 4ème étage HNB nord, CHU Hotel Dieu, 1 place Alexis Ricordeau, 44035 Nantes Cedex1, France. E-mail: patrick.baril@inserm.fr
Received 6 May 2009; revised 5 June 2009; accepted 15 June 2009

Table 1 Overview of imaging systems

Imaging modality[a]	*Resolution*	*Depth*	*Temporal resolution*	*Sensitivity*[b]	*Quantitative*	*Cost*[c]	*Clinical use*
MRI	10-100 μM	No limit	Minutes to hours	10^{-3} to 10^{-5} M	Yes	Most expensive	Yes
CT	50 μM	No limit	Minutes	no probes	No	Expensive	Yes
PET	1–2 mm	No limit	Minutes to hours	10^{-11} to 10^{-12} M	Yes	Most expensive	Yes
SPECT	1–2 mm	No limit	Minutes to hours	10^{-10} to 10^{-12} M	Yes	Most expensive	Yes
Bioluminescence	3–5 mm	cm	Minutes	10^{-15} to 10^{-17} M	No	Cheap	No
Fluorescence	2–3 mm	cm	Minutes to hour	10^{-9} to 10^{-12} M	No	Cheap	No

[a]Table adapted from Blasberg, 2003 and Vassaux and Groot-Wassink, 2003.
[b]Probe concentrations.
[c]Cost is based on purchase price of the imaging system.

(Doubrovin *et al.*, 2001) and provide alternative treatments (Barton *et al.*, 2008).

One of the fields that could most benefit from this technology is biotherapies. Biotherapies use reagents of biological origin (antibodies, viruses, bacteria) for therapeutic effect. Considering the complexity of these reagents, molecular imaging has the potential to provide unique information that will guarantee their biosafety in humans and provide a rationale for the future development of new generations of reagents. In this context, non-invasive imaging of gene expression is an attractive prospect, allowing precise, spaciotemporal measurements of gene expression in longitudinal studies involving gene transfer vectors (Vassaux and Groot-Wassink, 2003; Raty *et al.*, 2007). With the emergence of cell therapies in regenerative medicine, it is also possible to track cells injected into subjects. The monitoring of *in vivo* gene expression is critical for the evaluation of the success or failure of biotherapeutic approaches. Tissue sampling can provide useful information to monitor clinical response, but repeatedly performing biopsies on multiple tissues is inconvenient and impossible in patients. Hence, the assessment of samples is poorly reproducible and is limited by the inaccessibility of some internal organs. Thus, techniques for repeated, non-invasive imaging of therapeutic gene expression are highly desirable. To be applicable, the imaging technique should provide precise information about the location, magnitude and persistence of transgene expression over time.

Different imaging technologies to visualize gene expression have been developed or are under development. They can be classed into two groups, according to whether or not radioisotopes are used to obtain visual information (Table 1) (Blasberg, 2003; Serganova *et al.*, 2007).

The non-nuclear medicine group includes magnetic resonance imaging, bioluminescence and fluorescence imaging (Briat and Vassaux, 2006). These technologies are currently mostly used in laboratory studies but, in their current state of development, cannot realistically be applied to humans. The most widely used technique is bioluminescence imaging, which relies on the detection of light emitted by oxidation of the luciferin substrate upon catalysis by the luciferase enzyme (Sweeney *et al.*, 1999; Negrin and Contag, 2006). This reaction requires ATP, magnesium and oxygen. The bioluminescence emitted can be detected and amplified, revealing the sites of luciferase expression. In transgenic animals, this technology can be used to detect the activation of specific signalling pathways (Hamstra *et al.*, 2006; Briat and Vassaux, 2008). Fluorescence imaging using GFP has many advantages as GFP is easily introduced into cells via transfection and can be fused to other proteins allowing dynamic monitoring of cellular processes (Hadjantonakis *et al.*, 2003). However, both of these methodologies are poorly sensitive and have limited depth of penetration and resolution. The second group (e.g. nuclear medicine-based technologies) is based on the ability of scanners to detect and localize gamma ray emission from the decay of a radiotracer. PET and SPECT scanners and the gamma camera are the three main types of scanners used in nuclear medicine. These currently offer the greatest potential for translation into clinical applications (Vassaux and Groot-Wassink, 2003; Penuelas *et al.*, 2005). They are highly sensitive and provide good spatial resolution, especially when they are coupled by macroscopic imaging systems such as computed tomography. These technologies, however, require more expensive cameras, and radioactivity. Their uses and imaging modalities will be discussed in this review.

To image gene expression, a reporter gene and specific radio-labelled probes are required (Table 2) (Blasberg, 2003). The general principle is that, upon expression of the reporter gene, the biodistribution of a tracer molecule is altered, leading to its local concentration at the site of reporter gene expression (Vassaux and Groot-Wassink, 2003). Three types of reporter gene families are currently being developed, based on enzymatic activities (Tjuvajev *et al.*, 1996; 1998), the presence of specific receptors (Rogers *et al.*, 2005) or ionic transport mediated by membrane proteins (Groot-Wassink *et al.*, 2002; 2004a,b). As an example, HSV-1-*tk* is able to phosphorylate a freely diffusible, radio-labelled substrate which becomes trapped inside target cells when phosphorylated by the enzyme. This local accumulation of the radio-labelled tracer can be detected using nuclear imaging techniques, depending on the isotope used (Tjuvajev *et al.*, 1996; 1998) and has been developed for various applications (Koehne *et al.*, 2003).

In this review, we will focus on imaging technology exploiting NIS as a reporter gene. The first part of the review will describe the biological function of NIS. In the second part, we will discuss the imaging potential of NIS to monitor gene expression in the live subject using nuclear imaging technology. Direct application of NIS as a gene reporter for biotherapy purposes will be developed in a final section. We will emphasize in particular its potential in (i) image-guided radiotherapy; (ii) monitoring of gene and vector biodistribution; and (iii) trafficking of stem cells.

Table 2 Examples of human reporter genes, radiolabeled probes and imaging modalities

Class of reporter genes[a]	*Gene*	*Reporter probes*	*Imaging modalities*
Enzyme	HSV-1-tk	[$^{123,124,\ 125,131}$I]FIAU; [^{18}F]FEAU [^{18}F]GCV; [^{18}F]FPCV; [^{18}F]FHBG	Scintigraphy, PET, SPECT
	Luciferase	D-Luciferin	Bioluminescence
	TK2	[^{124}I]FIAU; [^{18}F]FEAU	SPECT, PET
	GFP	Fluorochromes	Fluorescence camera
Transporter	NIS	[^{123,124,131}I]NaI; [^{99m}Tc]pertechnetate [^{186,188}Re]perrhenate	Scintigraphy, PET, SPECT
	NET	[^{123}I]MIBG	Scintigraphy, SPECT
Receptor	SSTR2	[^{188}Re]P829, [^{99m}Tc]P829 [^{111}In]DTPA-D-Phe1-octreotide	Scintigraphy, PET
	D2 receptor	[^{18F}]FESP	PET

[a]Table adapted from Blasberg, 2003; Vassaux and Groot-Wassink, 2003; Briat and Vassaux, 2006 and Serganova *et al.*, 2007.
D2, dopamine receptor 2; FEAU, 2′-fluoro-5-ethyl-1-β-D-arabinofuranosyluracil; FESP, Fluoroethylspiperone; FHBG, fluoro-3-(hydroxymethyl)butyl] guanine; FIAU, 2′deoxy-2′-fluoro-1-beta -d-arabinofuranosyl-5- iodo-uridine; FPCV, fluoropenciclovir; GCV, ganciclovir; MIBG, metaiodobenzylguanidine; NET, Norepinephrine transporter; SSTR2, Somatostatin subtype 2; TK2, Mitochondrial thymidine kinase2.

The sodium-iodide symporter

Biological function

The sodium iodide symporter (NIS) is a member of the sodium/solute family of proteins composed of the sodium/glucose co-transporter (SLC5), the sodium/myo-inositol symporter (SMIT), the sodium/proline symporter (NPT), the sodium/multivitamin transporter (SMVT) and the high-affinity choline transporter (CHT). All of these proteins share the same biological function to transport molecules across a phospholipid membrane using an electrochemical gradient of sodium ions (Na+) as carrier and an ATP-driven pump (Jung, 2002).

NIS is present on the basolateral membrane of thyroid follicular cells and is responsible for the active transport of iodide into the thyroid gland. Its presence in thyrocytes is required for the synthesis of thyroid hormones, T_3 and T_4 (Kogai *et al.*, 2006). NIS co-transports sodium and iodide ions into the cells in a 2:1 (Na^+:I^-) ratio. The energy required for the transport of iodide against the cellular electrochemical gradient is generated via the sodium/potassium (Na^+/K^+) ATPase. Therefore, in the thyroid, NIS is inhibited by factors that reduce the activity of the Na^+/K^+ ATPase, such as ouabain, and also by molecules capable of competing with iodide transport, such as thiocyanate (SCN^-), perchlorate (ClO_4^-) and other anions. Within thyroid cells, iodide is transported into the thyroid colloid by passive transport across the apical plasma membrane, implicating two potential iodide transporters: pendrin and apical iodide transporter (AIT). In the colloid, iodide is oxidized by thyroid peroxidase enzyme (TPO) to form active iodine, which is incorporated into tyrosine residues of thyroglobulin molecules for the synthesis of the thyroid hormones, T3 and T4. Iodine is, therefore, trapped in the thyroid gland by organification (Kogai *et al.*, 2006).

In addition to its expression in the thyroid, NIS is detectable and active in the salivary glands, gastric mucosa and lactating mammary glands (Tazebay *et al.*, 2000; Kogai *et al.*, 2006). However, the level of expression of NIS is lower in these tissues than in thyroid tissues. As in the thyroid, NIS is capable of mediating iodide uptake in these other tissues and this process can be blocked by thiocyanate and perchlorate anions. In contrast to thyroid tissues, there is no long-term retention of iodine and the expression of NIS is not regulated by TSH (Tazebay *et al.*, 2000; Kogai *et al.*, 2006). This indicates that iodide organification is a particular and unique characteristic of the thyroid gland, which can not be easily transposed to other tissues. The physiological function of NIS in extra-thyroidal tissues is still unclear.

NIS cloning, structure and expression in normal cells

The rat NIS gene was first cloned and characterized in 1996 (Dai *et al.*, 1996), rapidly followed by the human NIS gene (hNIS) (Smanik *et al.*, 1996). The knowledge of the coding sequence of NIS was crucial to understanding the regulation of NIS in the thyroid and its implication in thyroid disorders and treatments. The hNIS gene encodes a 3.9 kb mRNA transcript coding for a glycoprotein of 643 amino acids with a molecular mass of 70 to 90 kDa, depending on post-translational modifications. NIS is a 13 transmembrane domain protein with an extracellular amino- and intracellular carboxy-terminus that has strong amino acid sequence homology with the mouse, rat and pig NIS proteins (82.8%, 83% and 84.1% respectively).

NIS expression and functional activity are regulated at many different levels, from transcriptional activation to post translational modifications. As thyroidal NIS is only functional in the basolateral membrane of thyroid follicular cells, subcellular shuttling and plasma membrane retention signals also control NIS activity (Kogai *et al.*, 2006).

Stimulation of NIS expression by TSH represents the main regulatory system of NIS expression in the thyroid. TSH is a 30 kDa glycoprotein that binds to its receptor, expressed on the basolateral membrane of thyroid follicular cells. Upon binding, the cAMP cell signalling pathway is activated, inducing downstream transcriptional activation of the NIS gene (Fenton *et al.*, 2008) and iodide uptake in TSH stimulated-cells (Riedel *et al.*, 2001). TSH was found also to control translocation and retention of NIS at the plasma membrane, providing an additional level of control of its activity (Riedel *et al.*, 2001; Ferreira *et al.*, 2005). NIS regulation by TSH-cAMP signalling is mediated to a large extent by an enhancer region (Fenton

et al., 2008) located upstream of the proximal promoter of the human NIS gene (Fenton *et al*., 2008). These regulatory domains contain binding sites for thyroid-selective transcription factors such as Pax-8 and TTF-1 as well as a cAMP-responsive element binding protein (CREB) (Taki *et al*., 2002; Fenton *et al*., 2008). In addition to TSH, IGF-1, retinoic acid, IFN-γ and direct activation of the PI3-kinase and p38 MAPK pathways were found to be involved in the regulation of NIS expression in thyroid, whereas in lactating breast and in breast cancer cells, prolactin enhances the expression of NIS (Pekary and Hershman, 1998; Filetti *et al*., 1999; Garcia and Santisteban, 2002; Arturi *et al*., 2005; Kogai *et al*., 2008). Conversely, thyroglobulin suppresses the expression of NIS mRNA and of other thyroid-specific genes such as TPO and TRs, providing a sensitive control of NIS activity in the thyroid (Kogai *et al*., 2006; Suzuki and Kohn, 2006).

NIS expression in thyroidal and non-thyroid cancer cells

Advanced but well-differentiated thyroid cancer has been treated successfully for more than 50 years with radioiodine (^{131}I) therapy (Siegel, 1999). This tumour type expresses high levels of NIS, although its expression is heterogeneous among the tumour, and expresses as well other thyroid-specific genes which are required for the organification of radioiodine (Saito *et al*., 1998; Wapnir *et al*., 2003; Lee *et al*., 2007). Consequently, upon injection of ^{131}I, thyroid tumour cells accumulate and retain radiodide resulting in tumour radioablation by emission of β-particles and γ-radiation.

For other thyroidal cancers, the potency of radioiodide treatment is directly related to the effective radiation dose delivered to the tumour. NIS expression in poorly differentiated thyroid cancer tissues is variable and in some cases is down-regulated as compared with normal thyroid tissues. Consequently, iodide uptake is diminished and radiotherapy is largely ineffective. However, this limitation could be overcome using TSH stimulation of the thyroid prior to radioiodide administration (Jarzab *et al*., 2003) or by using pharmacological agents such as lithium to prolong the biological half-life of iodide in thyroid tissues (Elisei *et al*., 2006).

Regarding non-thyroid cancer tissues, up to 83% of invasive human breast carcinomas expressed NIS, whereas normal breast tissues are negative for the expression of NIS (Wapnir *et al*., 2003). However, in two independent studies, only 20 to 25% of NIS-positive tumours showed functional iodide-radiotracer uptake. This could be explained by the fact that, in these malignant tissues, both plasma membrane-associated and intracellular cytoplasmic NIS have been reported (Wapnir *et al*., 2003). These studies emphasize that, as for non-differentiated thyroid cancer cells, NIS protein synthesis, modification and membrane targeting are important factors for high iodide uptake.

Molecular imaging of gene expression

Imaging detection methods to visualize NIS expression in vivo

Different modalities have been reported for imaging hNIS-expressing tissues. These include PET, scintigraphic imaging and SPECT. The main advantages of nuclear detection methods is that they offer increased sensitivity, allow temporal and spatial resolution and, importantly, are relevant in translation to use in human patients. Both PET and SPECT give quantitative and non-invasive information at the level of reporter gene expression.

Scintigraphic imaging

Planar scintigraphic images of radioisotope biodistribution are limited in their resolution and quantitative potential and, unlike SPECT and PET, do not permit a three-dimensional reconstruction of the image obtained (Blasberg, 2003; Serganova *et al*., 2007). This imaging modality is, however, straightforward and less expensive and has been used recently to visualize the activation of specific signalling pathways using NIS as reporter gene (Che *et al*., 2007; Kim *et al*., 2007a,b; Yeom *et al*., 2008).

PET imaging

The emission of positrons is an essential requirement for PET scanning. When the positrons emitted from the radioisotope collide with local neighbouring electrons, high-energy gamma (γ) rays are produced, which travel in opposite directions from the point of collision and can be detected by a γ camera surrounding the subject. Detectors form a ring around the subject (from which photons are emitted) and only process events that occur simultaneously. Reconstruction of three-dimensional images (probe distribution) from the raw data is performed by different mathematical methods. They differ in their resolution, resolution–noise ratio, contrast and required processing time. The most widely used positron-emitting isotopes are generally short lived. Isotopes with the shortest half-lives (e.g. 20 min for ^{11}C, 109 min for ^{18}F) have to be produced in cyclotrons near to the laboratory or hospital where tracer synthesis, transport and application take place, or have to be shipped by air. Small variations in timing have important consequences. However, isotopes with longer half-lives (e.g. 4.2 days for ^{124}I) can be produced further away from the eventual site of use. Because it is completely absorbed in the tissue, the energy received from positron-emitting isotopes is higher than the energy received from isotopes used in SPECT (Briat and Vassaux, 2006).

SPECT imaging

For NIS-expression imaging, SPECT uses detectors to identify individual photons emitted by isotopes such as $^{123}I^-$ or $^{99m}TcO_4^-$. The direction of a photon emitted is determined by fitting lead collimators between the source of emission and the detectors. These collimators stop all photons not travelling in a certain direction relative to the detector panel. Therefore, the collimator rejects the photons not travelling at a right angle to the detectors or through a pinhole. As a result, the sensitivity of SPECT is much lower than for PET devices (Briat and Vassaux, 2006). Endogenous p53 transcriptional activity has been visualized using a γ-camera and the hNIS as a reporter gene placed under the control of a p53-responsive promoter (Doubrovin *et al*., 2001). SPECT/CT images were obtained in nude mice before and after treatment with

adriamycin, a known activator of the p53 pathway, following an intravenous injection of [^{99m}Tc] pertechnetate. The images showed a clear increase in tracer uptake following treatment, which correlated with p53 activation and expression of its target genes. These results demonstrated the feasibility of monitoring the regulation of gene expression using SPECT. The SPECT imaging approach is readily adaptable to the clinic and has been widely used.

As for PET imaging, various manufacturers have developed small-animal SPECT imaging devices [microSPECT (Gamma Medica-Ideas), HiSPECT (Bioscan), and NanoSPECT (Bioscan)]. These systems, as it is the case for microSPECT (Carlson *et al.*, 2006), now offer good resolution and the possibility of being coupled with computerized tomography for anatomical imaging. In contrast to human studies, small-animal imaging requires a high spatial resolution because of the small size of the organism to be studied. This is achieved using pinhole collimators, which can be adapted to the γ-camera. In addition, multiple pinholes can be used to increase both the spatial resolution and sensitivity.

Applications in biotherapies

Biodistribution of gene transfer in gene therapy

Soon after the rat NIS gene was cloned in 1996 (Dai *et al.*, 1996), imaging of the transgene in non-thyroid cells was demonstrated by gamma camera (Shimura *et al.*, 1997). Lately, intra-tumoural injection of 2×10^9 infectious adenovirus particles encoding NIS was shown to be able to image tumour sites *in vivo* and to redirect 11% ID/g of the injected radioiodine to the tumour (Boland *et al.*, 2000). These first reports validated the use of NIS as a reporter gene for imaging gene expression in the live subject using non-invasive imaging technology. Since then, a large number of reports have been published (Boland *et al.*, 2000; Spitzweg *et al.*, 2000; Groot-Wassink *et al.*, 2002; 2004a; Barton *et al.*, 2003; Cho *et al.*, 2007; Raty *et al.*, 2007; Montiel-Equihua *et al.*, 2008) confirming the feasibility of the approach for small-animal imaging. Recently, non-invasive imaging of NIS expression upon viral gene transfer has been demonstrated as feasible and safe in humans (Barton *et al.*, 2008). In a phase I study, detection of gene transfer and persistence of gene expression in the whole body of patients with localized prostate cancer was imaged accurately using a SPECT/CT scanner and a replication-competent adenovirus armed with two suicide genes and NIS as the gene reporter. Data from nuclear imaging demonstrated in this study that intra-prostatic injection of 10^{12} viral particles led to the detection of NIS expression in the prostate in seven out of nine patients over a period of 7 days. Peak transgene expression, and therefore maximal viral spread, was detected 1 to 2 days after administration, covering on average 18% of the total volume of the prostate. Whole-body serial imaging of NIS expression in these patients indicated that there was no extra-prostatic dissemination of the virus, explaining in part the absence of serious adverse events observed. This study is first carried out in human patients and validates the use of NIS as a reporter gene for monitoring both gene and vector biodistribution in humans (Barton *et al.*, 2008).

Imaging using NIS has several advantages. Iodide is the radiotracer; therefore, radio-labelling and radiochemistry are not required, reducing costs. The imaging of NIS-expressing tissues is particularly versatile as NIS can promote the cellular uptake of different radioisotopes $^{123}I^-$ (SPECT), $^{124}I^-$ (PET), $^{99m}TcO_4^-$ (SPECT), $^{131}I^-$ (scintigraphic imaging) (Vassaux and Groot-Wassink, 2003). However, the lack of organification of iodide in extra-thyroidal tissues is a disadvantage using NIS as a reporter gene. There is a dynamic system of passive efflux of iodide and other NIS-specific radiotracers from cells transduced with NIS that produces difficulties in monitoring the process. The accumulation of iodide can be predicted to be a dynamic phenomenon, largely dependent on the clearance of the tracer, and for which the clearance effect will vary between organs. However, our laboratory (Groot-Wassink *et al.*, 2002; 2004b) and others (Boland *et al.*, 2000; Smit *et al.*, 2002; Haberkorn *et al.*, 2004) have shown that the rate of efflux of iodide is slow: 1 h after iodide injection, 5 to 7% of the injected dose is still present in the plasma (Groot-Wassink *et al.*, 2002; 2004b). The residual iodide was enough to allow concentration in NIS-expressing organs and to monitor precisely the localization of gene transfer. In another study, we (Groot-Wassink *et al.*, 2004b) took advantage of the high sensitivity and quantitative potential of PET scanning to assess whether gene transfer could provide quantitative information on gene expression in mice. Increasing doses of an adenovirus coding for NIS were injected intravenously into experimental mice before the administration of ^{124}I. Post-mortem γ counting of liver biopsies was found to be directly correlated with the dose of adenovirus injected and with both NIS mRNA concentration and the number of NIS-expressing cells detected in these tissues. In order to assess whether PET scanning could also gather accurate and quantitative information on gene expression, iodide uptake measured by PET was compared to post-mortem γ counting values. The results revealed a good correlation ($r^2 = 0.9581$) between the uptake value of ^{124}I detected in the liver by PET and the value detected by post-mortem γ counting (Groot-Wassink *et al.*, 2004b). These data provided evidence that PET measurements of iodide uptake are quantitative and provide accurate information to evaluate precisely the expression level of a therapeutic transgene in gene therapy approaches.

In addition to monitoring gene transfer mediated by viral vectors, nuclear imaging of NIS expression could be developed for use with new synthetic vector formulations. A synthetic vector could be defined as a nanoscale-size molecule with a chemical formulation allowing to stably entrap DNA to transfect efficiently targeted cells for DNA transgene expression. The majority of synthetic vectors are cationic, lipid-derived formulations and have been used successfully for *in vitro* transfection. This is in sharp contrast to the *in vivo* situation. Experimental data (Pack *et al.*, 2005; Cho *et al.*, 2007), obtained at autopsy of animals, have provided evidence that the diffusion of synthetic vectors in tumour masses is largely limited by non-specific absorption in the liver, lungs and kidneys and by macrophages of the reticuloendothelial system (Pack *et al.*, 2005; Cho *et al.*, 2007). This non-specific accumulation in healthy organs creates important toxicity issues and has largely hampered the widespread application of this type of gene delivery vehicle in the clinic. Recently, with

advances in the field of nanotechnology, PEG- or HPMA-modified polymeric nanoparticles have been shown to transform the size, charge and surface characteristics of the particles, resulting in longer circulation times in the blood, reduced uptake by the reticuloendothelial system and altered biodistribution in normal tissues (Pack *et al.*, 2005). Classically, biodistribution in mice is assessed by radioisotope-labelled nanoparticles followed by post-mortem radioactive counting and/or scintigraphic imaging. Therefore, to obtain final conclusive data for the identification of the best chemical formulation allowing high tumour targeting with limited diffusion in healthy organs, important radiochemistry and autopsy analyses are required. In this context, coupling a synthetic vector with an expression plasmid encoding hNIS could greatly reduce the cost and time of procedures and might also provide qualitative and quantitative information about the efficiency of gene transfer. In a recent study (Chisholm *et al.*, 2009), we demonstrated that a nanoparticle formulation composed of third generation polypropylenimine dendrimers, when complexed to hNIS plasmid, was capable of tumour transfection upon systemic administration to tumour-bearing mice. Whole-body nuclear imaging using a small-animal nano-SPECT/CT scanner and the human Na/I symporter (hNIS) as the reporter gene showed a unique and highly specific tumour targeting with no detection of gene transfer in any other tissues of tumour-bearing mice. Tumour-selective transgene expression was confirmed by quantitative RT-PCR at autopsy of scanned animals, while genomic PCR demonstrated that the tumour sites were the predominant sites of nanoparticle accumulation. Using this approach, we were able to demonstrate that the kinetic of NIS expression in tumours was transient. Peak of transgene expression was indeed detected 24 h after administration. Altogether, these data validated the use of the NIS as a reporter gene to monitor the exact biodistribution of gene transfer mediated by a synthetic vector, allowing the anticipation of potential toxicity issues.

Image-guided radiotherapy and dosimetry

In addition to its potential as an imaging transgene, NIS has therapeutic potential. These properties offer the unique possibility to combine the potential of nuclear imaging technology to provide precise, qualitative and quantitative information about gene expression with the potential of radiotherapy to kill cells expressing NIS by ionizing irradiation, as well as neighbouring cells through the physical cross-fire effect. The utilization of NIS in cancer gene therapy could lead to individualized therapy, as NIS expression upon gene transfer can be assessed in a living subject to determine the exact dose of radiation needed to efficiently irradiate tumour cells (Figure 1).

Experimentally, several groups have used gene therapy methodologies to transfer the NIS gene into non-thyroidal cancer cells to achieve a successful radioablation of the experimental tumour, as in differentiated thyroid cancer (Boland *et al.*, 2000; Spitzweg *et al.*, 2000; Dingli *et al.*, 2004; Dwyer *et al.*, 2005; 2006; Hasegawa *et al.*, 2006; Goel *et al.*, 2007; Montiel-Equihua *et al.*, 2008). Overall, the success of this approach resides in the level of NIS expression achieved in tumour cells as well as in the ability of tumour tissues to retain radioiodide within the cells. Because of their cellular origin, non-thyroidal cancer cells do not express endogenous TPO and are not capable of organifying iodide, even in the presence of exogenous hNIS. To overcome this problem, several approaches have been developed, with conflicting results. Some reports have demonstrated that co-expression of NIS with TPO (Huang *et al.*, 2001) or TIFF-1 (Furuya *et al.*, 2004) results in higher radioiodide uptake and retention by tumour cells, while another study (Boland *et al.*, 2002) reported that induced-iodide organification by TPO was not enough to increase the retention time of the radiotracer in target cells. Another promising approach consists of the identification of small molecules capable of influencing radioiodide uptake by NIS-expressing cells. A recent, high-throughput screening identified an imidazothiazole derivative component capable of increasing by 4.5-fold the retention of radioiodine in NIS-expressing cells (Lecat-Guillet *et al.*, 2007). Although these results are promising, dose-dependent experiments performed *in vitro* demonstrated that this component was capable of retaining iodide in NIS-expressing cells only when sub-micromolar concentrations of iodide were used (Lecat-Guillet and Ambroise, 2008). Considering the concentration of iodide in blood (10^{-8} to 10^{-9} M), this component is, therefore, unlikely to be effective *in vivo*. Thus, low or absent iodide organification in tissues remains a limiting factor in the use of NIS as a transgene for radiotherapy purposes. Indeed, the accumulation of iodide in cells has been demonstrated to be a dynamic process. Rapid efflux of iodide occurs through the cells when the radiotracer is removed from the extracellular medium. *In vivo*, a similar efflux of iodide takes place, although we (Groot-Wassink *et al.*, 2002; 2004b) and others (Boland *et al.*, 2000; Smit *et al.*, 2002; Haberkorn *et al.*, 2004) have demonstrated that iodide clearance is slow: There is still 5–7% ID/g of iodide in the plasma within 1 h after injection (Groot-Wassink *et al.*, 2004b). This circulating dose of the radiotracer in animals has been sufficient to eradicate experimental thyroidal and non-thyroidal tumour cells following hNIS expression. Interesting data from Faivre *et al.* (2004) indicate that iodide accumulation and retention is high in the liver without organification. Using chemically induced hepatocarcinomas model in rats, and injection of adenovirus encoding rat NIS directly into the liver portal vein, they observed a marked (20 to 30% of the injected dose) and sustained (>11 days) iodine uptake and retention in the hepatic tumours (Faivre *et al.*, 2004). Radioiodine therapy by injection of 650 MBq ^{131}I after gene transfer achieved a strong inhibition of tumour growth, complete regression of small nodules and prolonged survival of hepatocarcinoma-bearing rats. The sustained iodide uptake *in vivo* was attributed to permanent recycling of the effluent radioiodide via the hepatic blood flow and not to an active retention mechanism (Faivre *et al.*, 2004). Recently, Hingorani *et al.* demonstrated that radiation increased the magnitude and duration of NIS expression from replication-deficient adenoviruses (Hingorani *et al.*, 2008b). This effect was observed when various promoters were used to drive NIS expression and has important implications for future clinical applications. In another study, the same group demonstrated that the enhancement of transgene expression induced by the

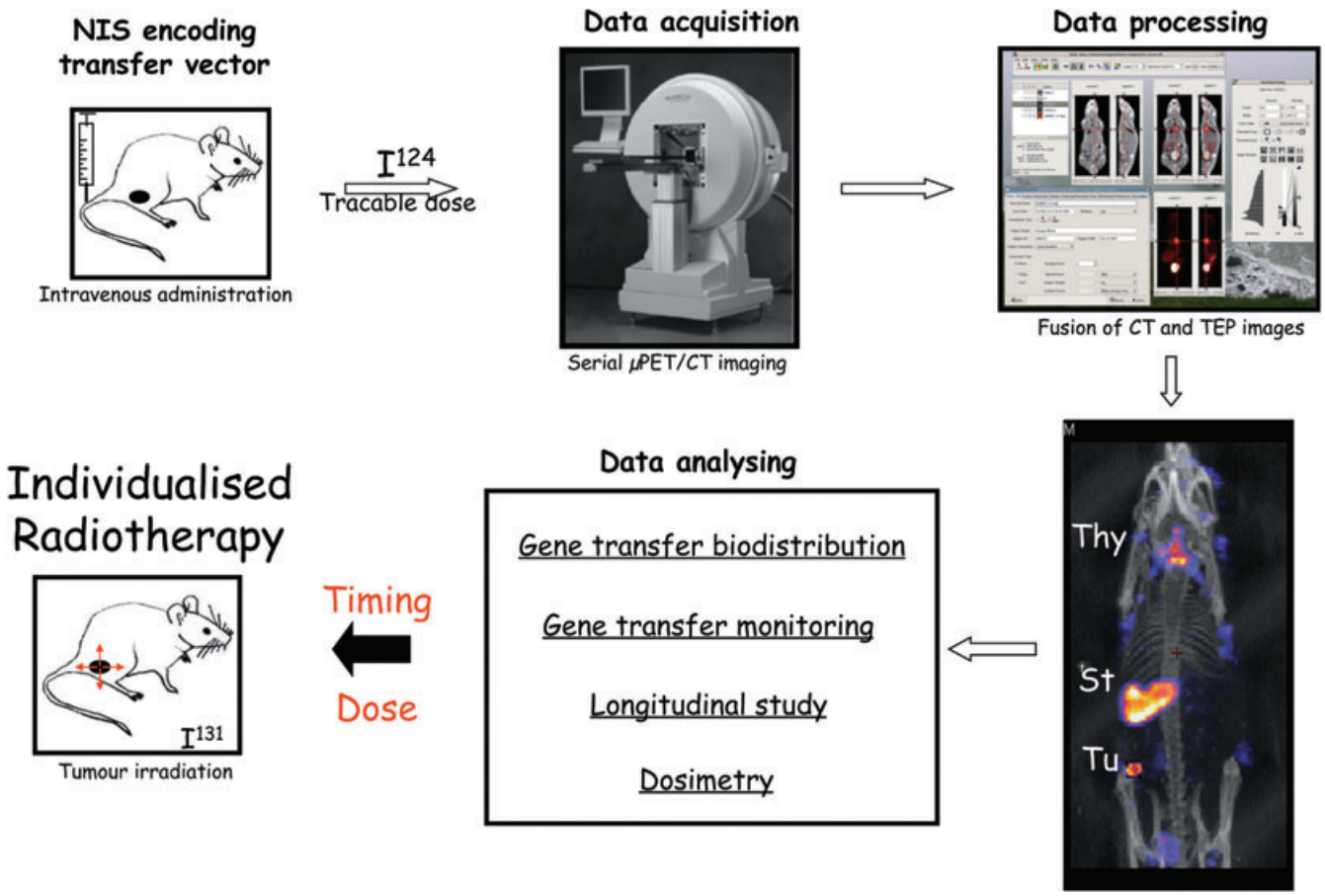

Figure 1 Schematic representation of the principle of image-guided radiotherapy mediated by NIS gene transfer in the living animal. Viral or synthetic gene transfer vectors encoding hNIS are injected intravenously into tumour-bearing mice. For kinetic studies, mice are anaesthetized, injected intravenously with radioiodide [^{124}I] and positioned in a µPET/CT scanner. PET images are obtained from various acquisition times depending on the specificity of radioactivity levels in mouse. A CT scan is taken at the same time. The reconstruction of images and fusion between PET and CT images are processed with adequate software such MEDISO and PMOD (Medical Imaging Systems). Final images are shown in coronal, axial or sagittal view in the plane of the tumour or, alternatively, as seen in this figure in three-dimensions (3D). Coloured dot points reveal radiotracer uptake in the whole body of mice while CT images allow the precise determination of the localization of the radiotracer emission source. In this example, radiotracer uptakes is detectable in the thyroid (Thy) and the stomach (St) as the result of endogenous expression of mNIS, and in the tumour (Tu) as the result of hNIS gene transfer. The kinetics of hNIS expression at the tumour site could be determined by quantification of the radiotracer activity in tumour tissues at different times in a longitudinal study carried out on the same animal. When expression of hNIS in the tumour is found to be maximal, a dosimetry study is then performed. Dosimetric calculation determines accurately the minimal therapeutic dose to administrate for selectively irradiated the tumour volume with minimal side effects. Such protocol fully validates the principle of individualized image-guided radiotherapy.

radiation was mediated in part by the formation of dsDNA breaks and subsequent MAPK pathway signalling, both *in vitro* and *in vivo* (Hingorani *et al.*, 2008a).

Various radioisotopes can be used in conjunction with NIS. Radioisotope species with greater energy deposition could also increase radiotherapy potency. NIS can promote cellular uptake of several isotopes such as Rhenium (Re) (Shen *et al.*, 2004) and Astatine (At) (Willhauck *et al.*, 2008). Rhenium (^{188}Re) is a β-emitter with a half-life of 16.7 h and a tissue penetration radius of 23–32 mm, making it particularly suitable for the treatment of large tumours. Dosimetry calculations indicate that ^{188}Re-perrhenate delivers up to a 4.5-fold higher dose of radioactivity than ^{131}I (Shen *et al.*, 2004). Astatine is a particularly attractive isotope for radiotherapy purposes. ^{211}At is an α-emitting radiohalide with a half-life of 7.2 h, tissue penetration of 60 µm and very high energy deposition. However, because of this short half-life and safety concerns, Astatine is not currently suitable for use in the clinic.

The successful treatment of NIS-expressing tumours with ^{131}I is likely to involve high radiotherapy doses which may be beyond to the limit of toxicity when scaled to use in human patients (Wenzel *et al.*, 2003). In the clinic, the most common approach to radionuclide dosimetry has been the MIRD S factor- (mean absorbed dose per unit cumulative activity) based method (Zanzonico, 2000). This approach is based on an algorithmic mathematical model which predicts the minimal, therapeutic, injected dose of a radioisotope required to irradiate tumour cells while sparing normal, healthy organs. As an example, the treatment of differentiated thyroid cancer has been carried out using fixed standard activities of I^{131} based on MIRD S factor software (Zanzonico, 2000). Although effective, this approach does not take into account the exact biokinetic distribution of the radioisotope within

the tumour, nor individual differences between tumour architecture, blood supply and tumour volume. As a result, the correlation between assessed doses and observed toxicities in targeted radiotherapy has not been completely satisfactory. Some patients have shown only partial tumour regression, while others have developed toxicity symptoms (Wiseman *et al.*, 2003). Therefore, accurate calculation of the therapeutic isotope dose to administer is a prerequisite for successful clinical response and safety. More recently, with advances in nuclear medicine imaging technology and the development of biophysical software, new dosimetric calculations have been made possible (Lassmann and Hanscheid, 2007). For example, three-dimensional imaging-based dosimetry methods combining ^{124}I PET images have allowed the acquisition of information on the spatial distribution of absorbed doses within a tumour, and the accurate determination of tumour volume and mean absorbed dose within a tumour. Data (Sgouros *et al.*, 2004) from a pilot study of a total of 56 patients with thyroid cancer showed high variability of ^{124}I uptake within thyroid tissues. The mean absorbed dose within individual patients was widely variable, ranging from 1.2 to 540 Gy, while the distribution of absorbed doses within individual tumours was also highly variable, ranging from a minimum of 0.3 Gy to a maximum of 4000 Gy. This study illustrated well the potential of NIS imaging to allow personalized therapy (Figure 1). Pre-therapy dosimetric calculations based on NIS imaging can allow very accurate estimations of the amount of radioisotope necessary to deliver a given dose of radiation to a particular tumour. Moreover, repeated radioisotope monitoring in tumours allows adjusting the ^{123}I therapeutic dose to administrate to the treated patient according to the tumour response. Finally, NIS-mediated radiotherapy could be combined with more classical external beam radiotherapy (Harrington *et al.*, 2008).

Image-guided radiovirotherapy

The development of molecular imaging strategies capable of monitoring the propagation of oncolytic viruses in tumours is crucial to obtain an optimal therapeutic effect. Clinical trials using oncolytic adenoviruses have emphasized that, although these genetically modified viruses are capable of replicating selectively in cancer cells, their therapeutic efficacy is limited (Waehler *et al.*, 2007). One reason for this is that virus spread within the tumour is often restricted to the initial site of infection. Viral propagation and potency are known to be prevented by intra-tumoural physical barriers such as stromal tissue composition, hypoxic and necrotic areas (Waehler *et al.*, 2007). A combination of the therapeutic potential of the oncolytic adenovirus with additional therapeutic intervention(s) is required to obtain greater tumour reduction. Combined use of oncolytic adenovirus with radiotherapy or conventional chemotherapy has been reported (Dilley *et al.*, 2005; Homicsko *et al.*, 2005; Cheong *et al.*, 2008). However, the mistimed combination of additional therapy has been described in preclinical studies (Wildner and Morris, 2000), resulting in loss of efficacy and even in virostatic effects. Therefore, the capability for non-invasive monitoring of virus spread in a tumour would provide unique information to rationalize the timing of these treatment combinations. Using two different engineered adenoviruses encoding NIS, and a small nano-SPECT/CT camera, we recently demonstrated that the kinetics of intratumoural spread could be monitored effectively *in vivo*. The peak of radiotracer uptake was detected 48 h post-infection for the first virus and at 72 h for the second one (Merron *et al.*, 2007). In addition, these data demonstrate that adenovirus replication in tumours is very transient and dependent on viral design. Of additional interest in the use of NIS for radiotherapy in combination with oncolytic viruses is the physical crossfire effect (Dingli *et al.*, 2004; Mitrofanova *et al.*, 2006). As the average path length of the β particle emitted by ^{131}I is 0.4 mm, non-transduced tumour cells could be destroyed by radiation emitted from neighbouring cells transduced by the recombinant oncolytic viruses expressing NIS. This effect can be particularly powerful (Dingli *et al.*, 2004; Mitrofanova *et al.*, 2006). Using an oncolytic measles virus, results from myeloma xenografts showed complete regression of the tumour after ^{131}I therapy even when only half of the tumour cells expressed NIS (Dingli *et al.*, 2004; Mitrofanova *et al.*, 2006).

Trafficking of cells with therapeutic potential

Another application of NIS as a gene reporter for imaging gene expression involves adoptive cell-based therapies. In this field, *in vitro* expansion of lymphocyte T cells with anti-tumour activity, followed by the re-implantation of these cells in the same patient, has been used for two decades with some clinical benefit, particularly for the treatment of melanoma (Rosenberg *et al.*, 2008). Although tumour T cell tropism was shown to be effective in patients, the exact biodistribution of these re-infused cells has not been characterized fully (Pittet *et al.*, 2007). In addition to T cells, other cell types such as mesenchymal stem cells, also exhibit a marked tropism for damaged areas including cancer tissues (Fritz and Jorgensen, 2008). Recently, mesenchymal stem cells have been the object of important research activity in the fields of both gene and cellular therapies. Promising results have been reported in graft versus host disease treatment, heart regeneration, cartilage and bone repair, skin wound healing and neuronal regeneration after strokes (Uccelli *et al.*, 2008). Mechanistically, inherent migration potential as well as their transdifferentiation property has been proposed as the cause of the plasticity of these cells. However, to date, there is insufficient information about the exact *in vivo* biodistribution, survival and biological comportment of these cells in targeted tissues (Uccelli *et al.*, 2008). In this context, constitutive expression of the hNIS gene in cells transduced with a lentiviral vector would provide a unique opportunity to study trafficking, homing and tumour targeting following injection of a radiotracer dose of I^{124}. Proof of principle of this approach has been demonstrated recently (Hwang *et al.*, 2008). The behaviour of stem cells incorporated into biocompatible chitosan or poly L-lactic acid (PLLA) scaffolds and then grafted subcutaneously in nude mice was visualized successfully using NIS as a gene reporter and a gamma camera as an imaging modality. Serial quantitative analyses of regions of interest drawn manually from the scintigraphy images demonstrated that radiotracer uptake by NIS-expressing stem cells was higher in cells grafted onto PLLA scaffolds than in cells not seeded onto a scaffold. Assuming

that NIS quantitative data are directly proportional to the number of viable cells, this imaging modality mediated by NIS allowed the identification in mice of the best scaffold polymeric structure capable of promoting efficient proliferation and survival of stem cells. This work provides a new rationale for the design of cell-scaffold complexes for tissue-regenerative and cell-replacement therapies (Hwang *et al.*, 2008). However, transduction of human patients with integrative vectors has been shown to lead to adverse events, in particular leukaemia (Hacein-Bey-Abina *et al.*, 2003). Therefore, besides imaging stem cell and other cell-type migration, the use of NIS as a gene reporter could also be exploited for the irradiation (I^{131}) of transduced, NIS-positive cells in the case of adverse events.

Moving towards clinical applications

Non-invasive imaging technology will help in the design and improvement of gene therapy applications. The capability to visualize and monitor *in vivo* the regulation of gene expression (either of endogenous genes or genes that have been delivered to cells using a viral, synthetic or cellular vector) in small animals will lead to novel therapeutic approaches in clinical research, as well as advances in the design of safe and efficient vectors such as viruses to be used in clinical settings. Among the safety issues, specific targeting of diseased sites is an important safety consideration for all trials involving patients. As NIS imaging has been validated recently in humans (Barton *et al.*, 2008), non-invasive molecular imaging will help clinicians to monitor *in vivo* the distribution and pharmacodynamics of gene expression in a precise and quantitative way.

Note

The drug and molecular target nomenclatures used in this manuscript are in agreement with the BJP's Guide to Receptors and Channels (Alexander *et al.*, 2008).

Acknowledgements

The work in the authors' laboratory is supported by grants from INSERM, la Ligue Nationale Contre le Cancer, ARC, and by grant 0607-3D1615-66/AO INSERM from the French National Cancer Institute (INCa). The publication of this article was possible with thanks to financial support brought by Association Française pour l'Etude du Foie and BMS laboratories.

Statement of conflict of interest

None.

References

Alexander SP, Mathie A, Peters JA (2008). Guide to Receptors and Channels (GRAC), 3rd edition. *Br J Pharmacol* **153** (Suppl. 2): S1–S209.

Arturi F, Ferretti E, Presta I, Mattei T, Scipioni A, Scarpelli D *et al.* (2005). Regulation of iodide uptake and sodium/iodide symporter expression in the MCF-7 human breast cancer cell line. *J Clin Endocrinol Metab* **90**: 2321–2326.

Barton KN, Stricker H, Brown SL, Elshaikh M, Aref I, Lu M *et al.* (2008). Phase I study of noninvasive imaging of adenovirus-mediated gene expression in the human prostate. *Mol Ther* **8**: 508–518.

Barton KN, Tyson D, Stricker H, Lew YS, Heisey G, Koul S *et al.* (2003). GENIS: gene expression of sodium iodide symporter for noninvasive imaging of gene therapy vectors and quantification of gene expression in vivo. *Mol Ther* **8**: 508–518.

Blasberg RG (2003). Molecular imaging and cancer. *Mol Cancer Ther* **2**: 335–343.

Boland A, Ricard M, Opolon P, Bidart JM, Yeh P, Filetti S *et al.* (2000). Adenovirus-mediated transfer of the thyroid sodium/iodide symporter gene into tumors for a targeted radiotherapy. *Cancer Res* **60**: 3484–3492.

Boland A, Magnon C, Filetti S, Bidart JM, Schlumberger M, Yeh P *et al.* (2002). Transposition of the thyroid iodide uptake and organification system in nonthyroid tumor cells by adenoviral vector-mediated gene transfers. *Thyroid* **12**: 19–26.

Briat A, Vassaux G (2006). Preclinical applications of imaging for cancer gene therapy. *Expert Rev Mol Med* **8**: 1–19.

Briat A, Vassaux G (2008). A new transgenic mouse line to image chemically induced p53 activation in vivo. *Cancer Sci* **99**: 683–698.

Carlson SK, Classic KL, Hadac EM, Bender CE, Kemp BJ, Lowe VJ *et al.* (2006). In vivo quantitation of intratumoral radioisotope uptake using micro-single photon emission computed tomography/computed tomography. *Mol Imaging Biol* **8**: 324–332.

Che J, Doubrovin M, Serganova I, Ageyeva L, Beresten T, Finn R *et al.* (2007). HSP70-inducible hNIS-IRES-eGFP reporter imaging: response to heat shock. *Mol Imaging* **6**: 404–416.

Cheong SC, Wang Y, Meng JH, Hill R, Sweeney K, Kirn D *et al.* (2008). E1A-expressing adenoviral E3B mutants act synergistically with chemotherapeutics in immunocompetent tumor models. *Cancer Gene Ther* **15**: 40–50.

Chisholm EJ, Vassaux G, Martin-Duque P, Chevre R, Lambert O, Pitard B *et al.* (2009). Cancer-specific transgene expression mediated by systemic injection of nanoparticles. *Cancer Res* **69**: 2655–2662.

Cho YW, Park SA, Han TH, Son DH, Park JS, Oh SJ *et al.* (2007). In vivo tumor targeting and radionuclide imaging with self-assembled nanoparticles: mechanisms, key factors, and their implications. *Biomaterials* **28**: 1236–1247.

Dai G, Levy O, Carrasco N (1996). Cloning and characterization of the thyroid iodide transporter. *Nature* **379**: 458–460.

Dilley J, Reddy S, Ko D, Nguyen N, Rojas G, Working P *et al.* (2005). Oncolytic adenovirus CG7870 in combination with radiation demonstrates synergistic enhancements of antitumor efficacy without loss of specificity. *Cancer Gene Ther* **12**: 715–722.

Dingli D, Peng KW, Harvey ME, Greipp PR, O'Connor MK, Cattaneo R *et al.* (2004). Image-guided radiovirotherapy for multiple myeloma using a recombinant measles virus expressing the thyroidal sodium iodide symporter. *Blood* **103**: 1641–1646.

Doubrovin M, Ponomarev V, Beresten T, Balatoni J, Bornmann W, Finn R *et al.* (2001). Imaging transcriptional regulation of p53-dependent genes with positron emission tomography in vivo. *Proc Natl Acad Sci USA* **98**: 9300–93005.

Dwyer RM, Bergert ER, O'Connor MK, Gendler SJ, Morris JC (2005). In vivo radioiodide imaging and treatment of breast cancer xenografts after MUC1-driven expression of the sodium iodide symporter. *Clin Cancer Res* **11**: 1483–1489.

Dwyer RM, Bergert ER, O'Connor MK, Gendler SJ, Morris JC (2006). Adenovirus-mediated and targeted expression of the sodium-iodide symporter permits in vivo radioiodide imaging and therapy of pancreatic tumors. *Hum Gene Ther* **17**: 661–668.

Elisei R, Vivaldi A, Ciampi R, Faviana P, Basolo F, Santini F *et al.* (2006). Treatment with drugs able to reduce iodine efflux

significantly increases the intracellular retention time in thyroid cancer cells stably transfected with sodium iodide symporter complementary deoxyribonucleic acid. *J Clin Endocrinol Metab* **91**: 2389–2395.

Faivre J, Clerc J, Gerolami R, Herve J, Longuet M, Liu B *et al*. (2004). Long-term radioiodine retention and regression of liver cancer after sodium iodide symporter gene transfer in Wistar rats. *Cancer Res* **64**: 8045–8051.

Fenton MS, Marion KM, Hershman JM (2008). Identification of cyclic adenosine 3′,5′-monophosphate response element modulator as an activator of the human sodium/iodide symporter upstream enhancer. *Endocrinology* **149**: 2592–2606.

Ferreira AC, Lima LP, Araujo RL, Muller G, Rocha RP, Rosenthal D *et al*. (2005). Rapid regulation of thyroid sodium-iodide symporter activity by thyrotrophin and iodine. *J Endocrinol* **184**: 69–76.

Filetti S, Bidart JM, Arturi F, Caillou B, Russo D, Schlumberger M (1999). Sodium/iodide symporter: a key transport system in thyroid cancer cell metabolism. *Eur J Endocrinol* **141**: 443–457.

Fritz V, Jorgensen C (2008). Mesenchymal stem cells: an emerging tool for cancer targeting and therapy. *Curr Stem Cell Res Ther* **3**: 32–42.

Furuya F, Shimura H, Miyazaki A, Taki K, Ohta K, Haraguchi K *et al*. (2004). Adenovirus-mediated transfer of thyroid transcription factor-1 induces radioiodide organification and retention in thyroid cancer cells. *Endocrinology* **145**: 5397–5405.

Garcia B, Santisteban P (2002). PI3K is involved in the IGF-I inhibition of TSH-induced sodium/iodide symporter gene expression. *Mol Endocrinol* **16**: 342–352.

Geus-Oei LF, Oyen WJ (2008). Predictive and prognostic value of FDG-PET. *Cancer Imaging* **8**: 70–80.

Goel A, Carlson SK, Classic KL, Greiner S, Naik S, Power AT *et al*. (2007). Radioiodide imaging and radiovirotherapy of multiple myeloma using VSV(Delta51)-NIS, an attenuated vesicular stomatitis virus encoding the sodium iodide symporter gene. *Blood* **110**: 2342–2350.

Groot-Wassink T, Aboagye EO, Glaser M, Lemoine NR, Vassaux G (2002). Adenovirus biodistribution and noninvasive imaging of gene expression in vivo by positron emission tomography using human sodium/iodide symporter as reporter gene. *Hum Gene Ther* **13**: 1723–1735.

Groot-Wassink T, Aboagye EO, Wang Y, Lemoine NR, Keith WN, Vassaux G (2004a). Noninvasive imaging of the transcriptional activities of human telomerase promoter fragments in mice. *Cancer Res* **64**: 4906–4911.

Groot-Wassink T, Aboagye EO, Wang Y, Lemoine NR, Reader AJ, Vassaux G (2004b). Quantitative imaging of Na/I symporter transgene expression using positron emission tomography in the living animal. *Mol Ther* **9**: 436–442.

Haberkorn U, Beuter P, Kubler W, Eskerski H, Eisenhut M, Kinscherf R *et al*. (2004). Iodide kinetics and dosimetry in vivo after transfer of the human sodium iodide symporter gene in rat thyroid carcinoma cells. *J Nucl Med* **45**: 827–833.

Hacein-Bey-Abina S, von Kalle C, Schmidt M, Le Deist F, Wulffraat N, McIntyre E *et al*. (2003). A serious adverse event after successful gene therapy for X-linked severe combined immunodeficiency. *N Engl J Med* **348**: 255–256.

Hadjantonakis AK, Dickinson ME, Fraser SE, Papaioannou VE (2003). Technicolour transgenics: imaging tools for functional genomics in the mouse. *Nat Rev Genet* **4**: 613–625.

Hamstra DA, Bhojani MS, Griffin LB, Laxman B, Ross BD, Rehemtulla A (2006). Real-time evaluation of p53 oscillatory behavior in vivo using bioluminescent imaging. *Cancer Res* **66**: 7482–7489.

Harrington KJ, Melcher A, Vassaux G, Pandha HS, Vile RG (2008). Exploiting synergies between radiation and oncolytic viruses. *Curr Opin Mol Ther* **10**: 362–370.

Hasegawa K, Pham L, O'Connor MK, Federspiel MJ, Russell SJ, Peng KW (2006). Dual therapy of ovarian cancer using measles viruses expressing carcinoembryonic antigen and sodium iodide symporter. *Clin Cancer Res* **12**: 1868–1875.

Hingorani M, White CL, Merron A, Peerlinck I, Gore ME, Slade A *et al*. (2008a). Inhibition of repair of radiation-induced DNA damage enhances gene expression from replication-defective adenoviral vectors. *Cancer Res* **68**: 9771–9778.

Hingorani M, White CL, Zaidi S, Merron A, Peerlinck I, Gore ME *et al*. (2008b). Radiation-mediated up-regulation of gene expression from replication-defective adenoviral vectors: implications for sodium iodide symporter gene therapy. *Clin Cancer Res* **14**: 4915–4924.

Homicsko K, Lukashev A, Iggo RD (2005). RAD001 (everolimus) improves the efficacy of replicating adenoviruses that target colon cancer. *Cancer Res* **65**: 6882–6890.

Huang M, Batra RK, Kogai T, Lin YQ, Hershman JM, Lichtenstein A *et al*. (2001). Ectopic expression of the thyroperoxidase gene augments radioiodide uptake and retention mediated by the sodium iodide symporter in non-small cell lung cancer. *Cancer Gene Ther* **8**: 612–618.

Hwang DW, Jang SJ, Kim YH, Kim HJ, Shim IK, Jeong JM *et al*. (2008). Real-time in vivo monitoring of viable stem cells implanted on biocompatible scaffolds. *Eur J Nucl Med Mol Imaging* **35**: 1887–1898.

Jarzab B, Handkiewicz-Junak D, Roskosz J, Puch Z, Wygoda Z, Kukulska A *et al*. (2003). Recombinant human TSH-aided radioiodine treatment of advanced differentiated thyroid carcinoma: a single-centre study of 54 patients. *Eur J Nucl Med Mol Imaging* **30**: 1077–1086.

Jung H (2002). The sodium/substrate symporter family: structural and functional features. *FEBS Lett* **529**: 73–77.

Kelly KA, Bardeesy N, Anbazhagan R, Gurumurthy S, Berger J, Alencar H *et al*. (2008). Targeted nanoparticles for imaging incipient pancreatic ductal adenocarcinoma. *PLoS Med* **5**: e85:0657–0668.

Kim HJ, Jeon YH, Kang JH, Lee YJ, Kim KI, Chung HK *et al*. (2007a). In vivo long-term imaging and radioiodine therapy by sodium-iodide symporter gene expression using a lentiviral system containing ubiquitin C promoter. *Cancer Biol Ther* **6**: 1130–1135.

Kim KI, Kang JH, Chung JK, Lee YJ, Jeong JM, Lee DS *et al*. (2007b). Doxorubicin enhances the expression of transgene under control of the CMV promoter in anaplastic thyroid carcinoma cells. *J Nucl Med* **48**: 1553–1561.

Koehne G, Doubrovin M, Doubrovina E, Zanzonico P, Gallardo HF, Ivanova A *et al*. (2003). Serial in vivo imaging of the targeted migration of human HSV-TK-transduced antigen-specific lymphocytes. *Nat Biotechnol* **21**: 405–413.

Kogai T, Taki K, Brent GA (2006). Enhancement of sodium/iodide symporter expression in thyroid and breast cancer. *Endocr Relat Cancer* **13**: 797–826.

Kogai T, Sajid-Crockett S, Newmarch L, Liu YY, Brent G (2008). Phosphoinositide-3-kinase (PI3K) inhibition induces sodium/iodide symporter expression (NIS) in rat thyroid cells and human papillary thyroid cancer Cells. *J Endocrinol* **199**: 243–252.

Lassmann M, Hanscheid H (2007). Spatial dose mapping for individualizing radioiodine treatment. *J Nucl Med* **48**: 2–4.

Lecat-Guillet N, Ambroise Y (2008). Enhanced iodide sequestration by 3-biphenyl-5,6-dihydroimidazo[2,1-b]thiazole in sodium/iodide symporter (NIS)-expressing cells. *ChemMedChem* **3**: 1211–1216.

Lecat-Guillet N, Merer G, Lopez R, Pourcher T, Rousseau B, Ambroise Y (2007). A 96-well automated radioiodide uptake assay for sodium/iodide symporter inhibitors. *Assay Drug Dev Technol* **5**: 535–5340.

Lee SJ, Choi KC, Han JP, Park YE, Choi MG (2007). Relationship of sodium/iodide symporter expression with I131 whole body scan uptake between primary and metastatic lymph node papillary thyroid carcinomas. *J Endocrinol Invest* **30**: 28–34.

Merron A, Peerlinck I, Martin-Duque P, Burnet J, Quintanilla M, Mather S *et al*. (2007). SPECT/CT imaging of oncolytic adenovirus propagation in tumours in vivo using the Na/I symporter as a reporter gene. *Gene Ther* **14**: 1731–1738.

Mitrofanova E, Unfer R, Vahanian N, Link C (2006). Rat sodium iodide

symporter allows using lower dose of 131I for cancer therapy. *Gene Ther* **13**: 1052–1056.

Montiel-Equihua CA, Martin-Duque P, de la Vieja A, Quintanilla M, Burnet J, Vassaux G, Lemoine NR (2008). Targeting sodium/iodide symporter gene expression for estrogen-regulated imaging and therapy in breast cancer. *Cancer Gene Ther* **15**: 465–473.

Negrin RS, Contag CH (2006). In vivo imaging using bioluminescence: a tool for probing graft-versus-host disease. *Nat Rev Immunol* **6**: 484–490.

Pack DW, Hoffman AS, Pun S, Stayton PS (2005). Design and development of polymers for gene delivery. *Nat Rev Drug Discov* **4**: 581–593.

Pekary AE, Hershman JM (1998). Tumor necrosis factor, ceramide, transforming growth factor-beta1, and aging reduce Na+/I-symporter messenger ribonucleic acid levels in FRTL-5 cells. *Endocrinology* **139**: 703–712.

Penuelas I, Haberkorn U, Yaghoubi S, Gambhir SS (2005). Gene therapy imaging in patients for oncological applications. *Eur J Nucl Med Mol Imaging* **32** (Suppl. 2): S384–S403.

Pittet MJ, Grimm J, Berger CR, Tamura T, Wojtkiewicz G, Nahrendorf M *et al.* (2007). In vivo imaging of T cell delivery to tumors after adoptive transfer therapy. *Proc Natl Acad Sci USA* **104**: 12457–12461.

Raty JK, Liimatainen T, Unelma Kaikkonen M, Grohn O, Airenne KJ, Yla-Herttuala S (2007). Non-invasive imaging in gene therapy. *Mol Ther* **15**: 1579–1586.

Riedel C, Levy O, Carrasco N (2001). Post-transcriptional regulation of the sodium/iodide symporter by thyrotropin. *J Biol Chem* **276**: 21458–21463.

Rogers BE, Parry JJ, Andrews R, Cordopatis P, Nock BA, Maina T (2005). MicroPET imaging of gene transfer with a somatostatin receptor-based reporter gene and (94m)Tc-Demotate 1. *J Nucl Med* **46**: 1889–1897.

Rosenberg SA, Restifo NP, Yang JC, Morgan RA, Dudley ME (2008). Adoptive cell transfer: a clinical path to effective cancer immunotherapy. *Nat Rev Cancer* **8**: 299–308.

Saito T, Endo T, Kawaguchi A, Ikeda M, Katoh R, Kawaoi A *et al.* (1998). Increased expression of the sodium/iodide symporter in papillary thyroid carcinomas. *J Clin Invest* **101**: 1296–1300.

Serganova I, Ponomarev V, Blasberg R (2007). Human reporter genes: potential use in clinical studies. *Nucl Med Biol* **34**: 791–807.

Sgouros G, Kolbert KS, Sheikh A, Pentlow KS, Mun EF, Barth A *et al.* (2004). Patient-specific dosimetry for 131I thyroid cancer therapy using 124I PET and 3-dimensional-internal dosimetry (3D-ID) software. *J Nucl Med* **45**: 1366–1372.

Shen DH, Marsee DK, Schaap J, Yang W, Cho JY, Hinkle G *et al.* (2004). Effects of dose, intervention time, and radionuclide on sodium iodide symporter (NIS)-targeted radionuclide therapy. *Gene Ther* **11**: 161–169.

Shimura H, Haraguchi K, Miyazaki A, Endo T, Onaya T (1997). Iodide uptake and experimental 131I therapy in transplanted undifferentiated thyroid cancer cells expressing the Na+/I- symporter gene. *Endocrinology* **138**: 4493–4496.

Siegel E (1999). The beginnings of radioiodine therapy of metastatic thyroid carcinoma: a memoir of Samuel M. Seidlin, M.D. (1895–1955) and his celebrated patient. *Cancer Biother Radiopharm* **14**: 71–79.

Smanik PA, Liu Q, Furminger TL, Ryu K, Xing S, Mazzaferri EL *et al.* (1996). Cloning of the human sodium iodide symporter. *Biochem Biophys Res Commun* **226**: 339–345.

Smit JW, Schroder-van der Elst JP, Karperien M, Que I, Stokkel M, van der Heide D *et al.* (2002). Iodide kinetics and experimental (131)I therapy in a xenotransplanted human sodium-iodide symporter-transfected human follicular thyroid carcinoma cell line. *J Clin Endocrinol Metab* **87**: 1247–1253.

Spitzweg C, O'Connor MK, Bergert ER, Tindall DJ, Young CY, Morris JC (2000). Treatment of prostate cancer by radioiodine therapy after tissue-specific expression of the sodium iodide symporter. *Cancer Res* **60**: 6526–6530.

Suzuki K, Kohn LD (2006). Differential regulation of apical and basal iodide transporters in the thyroid by thyroglobulin. *J Endocrinol* **189**: 247–255.

Sweeney TJ, Mailander V, Tucker AA, Olomu AB, Zhang W, Cao Y *et al.* (1999). Visualizing the kinetics of tumor-cell clearance in living animals. *Proc Natl Acad Sci USA* **96**: 12044–12049.

Taki K, Kogai T, Kanamoto Y, Hershman JM, Brent GA (2002). A thyroid-specific far-upstream enhancer in the human sodium/iodide symporter gene requires Pax-8 binding and cyclic adenosine 3′,5′-monophosphate response element-like sequence binding proteins for full activity and is differentially regulated in normal and thyroid cancer cells. *Mol Endocrinol* **16**: 2266–2282.

Tazebay UH, Wapnir IL, Levy O, Dohan O, Zuckier LS, Zhao QH *et al.* (2000). The mammary gland iodide transporter is expressed during lactation and in breast cancer. *Nat Med* **6**: 871–888.

Tjuvajev JG, Finn R, Watanabe K, Joshi R, Oku T, Kennedy J *et al.* (1996). Noninvasive imaging of herpes virus thymidine kinase gene transfer and expression: a potential method for monitoring clinical gene therapy. *Cancer Res* **56**: 4087–4095.

Tjuvajev JG, Avril N, Oku T, Sasajima T, Miyagawa T, Joshi R *et al.* (1998). Imaging herpes virus thymidine kinase gene transfer and expression by positron emission tomography. *Cancer Res* **58**: 4333–4341.

Uccelli A, Moretta L, Pistoia V (2008). Mesenchymal stem cells in health and disease. *Nat Rev Immunol* **8**: 726–736.

Vassaux G, Groot-Wassink T (2003). In vivo noninvasive imaging for gene therapy. *J Biomed Biotechnol* **2003**: 92–101.

Waehler R, Russell SJ, Curiel DT (2007). Engineering targeted viral vectors for gene therapy. *Nat Rev Genet* **8**: 573–587.

Wapnir IL, van de Rijn M, Nowels K, Amenta PS, Walton K, Montgomery K *et al.* (2003). Immunohistochemical profile of the sodium/iodide symporter in thyroid, breast, and other carcinomas using high density tissue microarrays and conventional sections. *J Clin Endocrinol Metab* **88**: 1880–1888.

Wenzel A, Upadhyay G, Schmitt TL, Loos U (2003). Iodination of proteins in TPO transfected thyroid cancer cells is independent of NIS. *Mol Cell Endocrinol* **213**: 99–108.

Wildner O, Morris JC (2000). The role of the E1B 55 kDa gene product in oncolytic adenoviral vectors expressing herpes simplex virus-tk: assessment of antitumor efficacy and toxicity. *Cancer Res* **60**: 4167–4174.

Willhauck MJ, Samani BR, Wolf I, Senekowitsch-Schmidtke R, Stark HJ, Meyer GJ *et al.* (2008). The potential of (211)Astatine for NIS-mediated radionuclide therapy in prostate cancer. *Eur J Nucl Med Mol Imaging* **35**: 1272–1281.

Wiseman GA, Kornmehl E, Leigh B, Erwin WD, Podoloff DA, Spies S *et al.* (2003). Radiation dosimetry results and safety correlations from 90Y-ibritumomab tiuxetan radioimmunotherapy for relapsed or refractory non-Hodgkin's lymphoma: combined data from 4 clinical trials. *J Nucl Med* **44**: 465–474.

Yeom CJ, Chung JK, Kang JH, Jeon YH, Kim KI, Jin YN *et al.* (2008). Visualization of hypoxia-inducible factor-1 transcriptional activation in C6 glioma using luciferase and sodium iodide symporter genes. *J Nucl Med* **49**: 1489–1497.

Zanzonico PB (2000). Internal radionuclide radiation dosimetry: a review of basic concepts and recent developments. *J Nucl Med* **41**: 297–308.